REPORT

Mutations in *PGAP3* Impair GPI-Anchor Maturation, Causing a Subtype of Hyperphosphatasia with Mental Retardation

Malcolm F. Howard,[1,13] Yoshiko Murakami,[2,3,13] Alistair T. Pagnamenta,[1,13] Cornelia Daumer-Haas,[4] Björn Fischer,[5,7] Jochen Hecht,[6,7] David A. Keays,[8] Samantha J.L. Knight,[1] Uwe Kölsch,[9] Ulrike Krüger,[5] Steffen Leiz,[10] Yusuke Maeda,[2,3] Daphne Mitchell,[11] Stefan Mundlos,[5,6,7] John A. Phillips III,[11] Peter N. Robinson,[5,6,7] Usha Kini,[12,14,*] Jenny C. Taylor,[1,14] Denise Horn,[5,14] Taroh Kinoshita,[2,3,14] and Peter M. Krawitz[5,6,7,14,*]

Glycosylphophatidylinositol (GPI)-anchored proteins play important roles in many biological processes, and mutations affecting proteins involved in the synthesis of the GPI anchor are reported to cause a wide spectrum of intellectual disabilities (IDs) with characteristic additional phenotypic features. Here, we describe a total of five individuals (from three unrelated families) in whom we identified mutations in *PGAP3*, encoding a protein that is involved in GPI-anchor maturation. Three siblings in a consanguineous Pakistani family presented with profound developmental delay, severe ID, no speech, psychomotor delay, and postnatal microcephaly. A combination of autozygosity mapping and exome sequencing identified a 13.8 Mb region harboring a homozygous c.275G>A (p.Gly92Asp) variant in *PGAP3* region 17q11.2–q21.32. Subsequent testing showed elevated serum alkaline phosphatase (ALP), a GPI-anchored enzyme, in all three affected children. In two unrelated individuals in a cohort with developmental delay, ID, and elevated ALP, we identified compound-heterozygous variants c.439dupC (p.Leu147Profs*16) and c.914A>G (p.Asp305Gly) and homozygous variant c.314C>G (p.Pro105Arg). The 1 bp duplication causes a frameshift and nonsense-mediated decay. Further evidence supporting pathogenicity of the missense mutations c.275G>A, c.314C>G, and c.914A>G was provided by the absence of the variants from ethnically matched controls, phylogenetic conservation, and functional studies on Chinese hamster ovary cell lines. Taken together with recent data on *PGAP2*, these results confirm the importance of the later GPI-anchor remodelling steps for normal neuronal development. Impairment of PGAP3 causes a subtype of hyperphosphatasia with ID, a congenital disorder of glycosylation that is also referred to as Mabry syndrome.

Glycosylphophatidylinositol (GPI) anchoring is a post-translational modification that tethers proteins to plasma membranes, and it is thought to play a role in protein sorting and trafficking.[1] The GPI anchor is well conserved among eukaryotes, and there are over 150 mammalian GPI-anchored proteins (GPI-APs), including receptors, adhesion molecules, and enzymes.[1] Many of these proteins are critical for normal neural and embryonic development.[2,3] There are around 30 genes known to be involved in the biosynthesis and remodelling of the GPI anchor, which is formed in the endoplasmic reticulum (ER), where it is attached by the GPI transamidase to a protein showing a specific C-terminal signal before it is transported to the Golgi apparatus for fatty acid remodelling and cellular export.

In the last 4 years, germline mutations in eight genes selectively involved in the GPI-anchor-synthesis pathway have been shown to cause a wide phenotypic spectrum of disorders with intellectual disability (ID) and seizures; these range from syndromic forms with characteristic malformations and minor anomalies to nonsyndromic forms. Congenital disorders that are caused by an impairment of GPI-anchor synthesis and maturation are now classified as congenital disorders of glycosylation (CDGs), a diverse class of metabolic diseases.[4]

PIGV (MIM 610274), *PIGO* (MIM 614730), and *PGAP2* (MIM 615187), three different genes in the GPI-anchor-synthesis pathway, have been implicated in hyperphosphatasia with mental retardation syndrome (HPMRS [MIM 239300]), also known as Mabry syndrome, a recently delineated autosomal-recessive form of ID with a distinct facial dysmorphism, consistently elevated serum alkaline phosphatase (ALP) (hyperphosphatasia), brachytelephalangy, and seizures. All individuals with congenital impairment of GPI-anchor synthesis have residual surface levels of GPI-anchored proteins, and it is hypothesized that complete-loss-of-function mutations in genes involved with GPI-anchor synthesis are embryonically lethal.[5]

[1]National Institute for Health Research Biomedical Research Centre, Wellcome Trust Centre for Human Genetics, University of Oxford, OX3 7BN Oxford, UK; [2]Department of Immunoregulation, Research Institute for Microbial Diseases, Osaka University, Osaka 565-0871, Japan; [3]World Premier International Immunology Frontier Research Center, Osaka University, Osaka 565-0871, Japan; [4]Pränatal-Medizin München, 80637 München, Germany; [5]Institute for Medical Genetics and Human Genetics, Charité Universitätsmedizin, 13353 Berlin, Germany; [6]Berlin Brandenburg Center for Regenerative Therapies, Charité Universitätsmedizin, 13353 Berlin, Germany; [7]Max Planck Institute for Molecular Genetics, 14195 Berlin, Germany; [8]Research Institute of Molecular Pathology, 1030 Vienna, Austria; [9]Institute of Medical Immunology, Charité Universitätsmedizin, 13353 Berlin, Germany; [10]Department of Pediatrics, Klinikum Dritter Orden, 80638 München, Germany; [11]Division of Medical Genetics and Genomic Medicine, Department of Pediatrics, Vanderbilt University School of Medicine, TN 37232-2578, USA; [12]Department of Clinical Genetics, Oxford University Hospitals NHS Trust, OX3 9DU Oxford, UK
[13]These authors contributed equally to this work
[14]These authors contributed equally to this work and are co-senior authors
*Correspondence: usha.kini@ouh.nhs.uk (U.K.), peter.krawitz@charite.de (P.M.K.)
http://dx.doi.org/10.1016/j.ajhg.2013.12.012.

The effect of mutations causing GPI-anchor deficiencies can be subdivided into groups on the basis of the serum activity of the marker enzyme ALP. Mutations in *PIGA* (MIM 311770), *PIGL* (MIM 605947), *PIGM* (MIM 610273), *PIGN* (MIM 606097), and *PIGT* (MIM 610272) affect early GPI-anchor synthesis and the attachment of proteins to the GPI anchor.[6–10] These variants result in primary reduced surface levels of GPI-APs because of their increased intracellular degradation and are not associated with high serum ALP. Mutations in *PIGV* and *PIGO* affect late GPI-anchor synthesis.[11,12] However, GPI transamidase recognizes the incomplete GPI anchor and cleaves the GPI attachment signal, leading to the generation of non-GPI-anchored soluble proteins.[13] Individuals with mutations in *PIGV* and *PIGO* have primary reduced GPI-AP surface levels as a result of increased secretion into the extracellular space, resulting in high serum ALP. Recently, mutations in *PGAP2* have been reported to affect the final GPI-anchor fatty-acid-remodelling step and to thus result in abnormal GPI-APs that are more prone to cleavage.[14–16] Individuals with *PGAP2* mutations have secondary reduced GPI-AP surface levels also as a result of increased secretion into the extracellular space, resulting in high serum ALP. GPI remodelling occurs in the Golgi and involves the removal of an unsaturated fatty acid at the sn-2 position by PGAP3 and its subsequent substitution with a saturated fatty acid by PGAP2. Fatty acid remodelling is critical for proper association between GPI-APs and lipid rafts.[17]

A number of deficient GPI-pathway genes were first identified via traditional autozygosity mapping in combination with next-generation sequencing methodologies.[10,14] This methodology has become a key strategy for the identification of disease-associated genes, particularly those related to genetically heterogeneous conditions such as ID, and was the approach taken for the first family described here.[18]

Family A originates from the Sargodha district of Punjab in Pakistan. The parents are second cousins, and all three children (Figures 1A and 2A) presented with profound developmental delay, severe learning disability, no speech, psychomotor delay, and postnatal microcephaly (−2 to −3 SDs) at the ages of 17, 8, and 4 years. Further clinical details are summarized in Table 1. After a *ASPM* test that did not detect pathogenic variants, they were recruited into the ongoing Structural Brain Abnormalities and Learning Disabilities Study (see Oxford Brain Abnormality Research Group in Web Resources), which received UK ethics approval from the Wales Research Ethics Committee (12/WA/0001) and obtained informed consent from the responsible persons on behalf of all study participants. Blood DNA samples for IV-2, IV-3, V-1, V-2, and V-3 were run on CytoSNP12v2 arrays (Illumina), which confirmed familial relationships and that there were no copy-number changes of likely clinical relevance (Table S1, available online). Autozygosity mapping was then used for identifying a single 13.8 Mb candidate region in 17q11.2–q21.32 (Figure S1). None of the 359 annotated genes appeared to be obvious candidates, and so an exome sequencing approach was adopted.

The exome of proband V-2 was enriched (TruSeq, Illumina) and sequenced on a HiSeq2500 (Illumina) with the use of standard settings and the 100 bp paired-end read format. Reads were mapped to the human reference sequence (UCSC Genome Browser, hg19) with the use of Stampy,[19] and variants were called with Platypus. The resulting VCF file was uploaded into Ingenuity Variant Analysis (v.2.1.20130711) and filtered for rare variants that were in the homozygous region on chromosome 17 and predicted to be deleterious (Table S2 and Web Resources).

The single remaining variant was a c.275G>A change in *PGAP3* (RefSeq accession number NM_033419.3). Sanger sequencing confirmed that this variant cosegregated with disease, consistent with an autosomal-recessive mode of inheritance (Figure 1B). The variant is predicted to cause a p.Gly92Asp alteration to the protein sequence at a highly conserved position (Figure 1C) and is not present at any frequency in the NHLBI Exome Sequencing Project Exome Variant Server (EVS), 1000 Genomes (version 3), or 274 in-house genomes of mixed ancestry. The mutation was also not detected in 108 Punjabi individuals from Lahore, suggesting that c.275G>A is unlikely to be a variant specific to this ethnicity.

In parallel, we performed targeted sequencing in 19 individuals with ID and elevated ALP and in whom HPMRS was suspected. The Charité University Medicine ethics board approved this study, and we obtained informed consent from the responsible persons (parents) on behalf of all study participants. After excluding pathogenic *PIGV* mutations that are the most common cause of HPMRS by Sanger sequencing, we subjected DNA to enrichment of all 30 known genes associated with GPI-anchor synthesis by using a customized SureSelect library (Agilent), as well as subsequent sequencing on a HiSeq2000, as previously described.[15] Sequence variants were filtered under an autosomal-recessive model of inheritance in GeneTalk,[20] which yielded potentially pathogenic variants in *PGAP3* in two individuals. Compound-heterozygous variants c.439dupC (p.Leu147Profs*16) and c.914A>G (p.Asp305Gly) were detected in individual II-1 from family B, and homozygous variant c.314C>G (p.Pro105Arg) was identified in individual II-1 from family C (Figure 1B).

The detailed clinical findings of individual II-1 from family B were reported previously (affected individual 4 in Thompson et al.)[21] together with a single rare heterozygous variant in *PIGV*, c.1369C>T.[21] However, in *PIGV*-defective Chinese hamster ovary (CHO) cells, the altered protein restored the surface levels of GPI-APs as efficiently as the wild-type protein, suggesting no functional impairment of *PIGV* (Figure S4). In contrast, the duplication of c.439dupC in *PGAP3* causes a frameshift that introduces a premature stop codon, most likely resulting in nonsense-mediated decay of the transcript. To exclude further candidate mutations, we exome sequenced DNAs of the affected

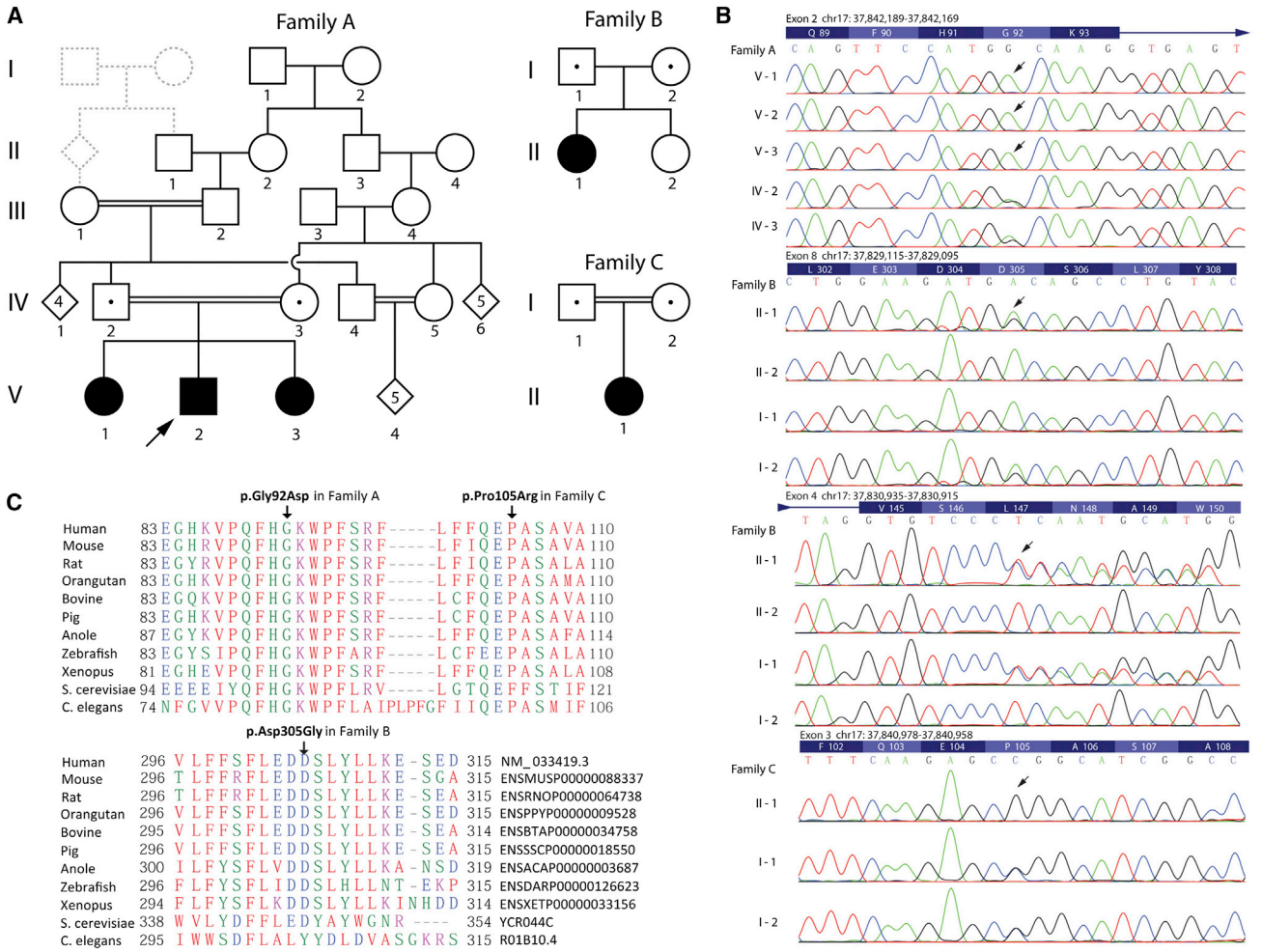

Figure 1. Pedigrees, Sanger Validation, and Phylogenetic Conservation of the Variant Filtering Cascade and Molecular Characterization of *PGAP3* Mutations

(A) Pedigrees are shown for family A (of Pakistani descent), family B (of European descent), and family C (of Saudi Arabian origin). Shading indicates ID and hyperphosphatasia, and proven heterozygote carriers are shown by a dot. In family A, the gray dotted lines indicate an additional consanguineous loop that was not described in the clinical notes but that was inferred by the high inbreeding coefficient detected in IV-2 from the SNP array data. The proband is indicated with an arrow.

(B) Sanger validation and segregation testing of *PGAP3* variants. DNA for the unaffected double first cousins in family A (collectively labeled as V-4) was not available.

(C) ClustalW alignment of amino acid sequence shows high evolutionary conservation.

individual of family B and her parents and confirmed the compound-heterozygous variants in *PGAP3* as the only candidate mutations for an autosomal-recessive model of inheritance.[22,23]

Individual II-1 of family B is the first child of nonconsanguineous European-American parents (Table 1 and Figures 1A and 2B). Her psychomotor development was severely delayed, and she developed tonic-clonic seizures. Physical examination at the age of 10 years showed postnatal short stature, dystrophy, normal occipitofrontal circumference (OFC), and dysmorphic facial features. ALP levels were repeatedly elevated, and a GPI-anchor deficiency on granulocytes and monocytes could be measured by flow cytometry with CD16, CD24, and fluorescence-labeled aerolysin staining (Figure 3A). In family C, individual II-1 is the first child of consanguineous parents of Saudi Arabian origin (Table 1 and Figures 1A and 2C). She had severe psychomotor delay. Myoclonic seizures started in her second year of life. Physical examination of this 2-year-old female showed normal growth parameters and OFC but axial muscular hypotonia, uncoordinated movements, and facial dysmorphism. ALP activity was elevated in repeated tests. Sanger sequencing confirmed that the parents are heterozygous for c.314C>G, and the mutation was not detected in 52 Arabic controls or the NHLBI Exome Sequencing Project EVS, suggesting that it might be a private mutation specific to this family (Figure 1B).

The most common features noted in all affected individuals were normal growth parameters and OFC at birth, severe psychomotor delay with no speech and marked motor delay, and characteristic facial features. Four were unable to walk, whereas the other began to walk with support at the age of 3. Seizures starting between the ages of 18 months and 12 years developed in four of five affected

Figure 2. Photographs of Affected Individuals
Facial features seen in (A) individual V-3 from family A, (B) individual II-1 from family B, and (C) individual II-1 from family C at the ages of 4, 10, and 2 years, respectively. These individuals bear a striking resemblance with a broad nasal bridge, long-appearing palpebral fissures, a broad nasal tip, a short nose, a long philtrum, a thin and wide upper lip, full cheeks, and large fleshy ear lobes.

individuals. Three were described as having tonic-clonic seizures, and the other had myoclonic seizures. Consistent ALP elevation varied between 1.4 and 5 times the age-adjusted upper limit of the normal range. The facial gestalt was similar to that of individuals with HPMRS and included features such as a broad nasal bridge, a short nose with a broad nasal tip, a thin and wide upper lip, and large fleshy ear lobes. In contrast, postnatal development of head circumference and growth parameters differed among the affected individuals studied here. Affected individuals in family A developed microcephaly, whereas OFC was in the mean range in the other individuals. In the affected individual from family B, marked short stature was present, whereas the other affected individuals had a mean height according to age. Two of five individuals had cleft palate, whereas abnormal MRI findings such as thin corpus callosum and dilated lateral ventricles were observed in the affected individual from family C.

The common features of all individuals reported with mutations in *PIGV*, *PIGO*, *PGAP2*, and *PGAP3* are severe psychomotor delay and ID, epilepsy, elevated ALP, and a distinctive facial gestalt. In contrast, brachytelephalangy, which is an important diagnostic sign in other types of HPMRS, is not present in any affected individuals with *PGAP3* mutations. Marked variability regarding the postnatal growth and OFC has also been observed in the groups of affected individuals carrying *PIGV*, *PIGO*, and *PGAP2* mutations. Also, cleft palate has been previously documented in other individuals with HPMRS due to mutations in these genes. In individuals affected by HPMRS and mutations in genes other than *PGAP3*, associated malformations seem to appear more frequently and their spectrum seems to be broader.

To determine the functional consequences of the four *PGAP3* mutations, we used a mutant CHO cell line defective in both *PGAP3* and *PGAP2* (see Figure S3 for principles of the assay).[17] The mutant cells have GPI-APs at mildly reduced levels because of a lack of GPI fatty acid remodelling. When wild-type *PGAP3* cDNA was transfected, the first step in the fatty acid remodelling was restored, whereas the second step remained defective, leading to the release of lyso-GPI intermediates and resulting in a severe reduction in the surface levels of GPI-APs (Figure 3Bi). If the mutant *PGAP3* cDNA has decreased activity, reduction in the surface GPI-AP levels would be partial. Mutant *PGAP3* cDNA bearing the mutation found in family A (c.275G>A [p.Gly92Asp]) either did not reduce or reduced only slightly the surface levels of three GPI-APs: CD59, CD55 (DAF), and urokinase plasminogen activator receptor (uPAR), indicating that the substitution caused a null or nearly null phenotype (Figure 3Bii). One of the substitutions found in family B (p.Leu147Profs*16) also caused a null phenotype, whereas the other (p.Asp305Gly) significantly reduced levels of all three GPI-APs, indicating some residual activity (Figure 3Biii). The substitution found in family C (p.Pro105Arg) caused less efficient reduction of GPI-APs than did the p.Asp305Gly substitution in family B, indicating an even lower residual activity (Figure 3Biv).

To clarify the mechanisms of these functional losses, we expressed mutant *PGAP3* clones that were hemagglutinin (HA) tagged at the N terminus in CHO cells and analyzed them by SDS-PAGE and immunoblotting (Figure 4) and immunofluorescence microscopy (Figure 5) with anti-HA. On SDS-PAGE and immunoblotting, HA-PGAP3 appeared as a smear band at around 37–45 kDa and several clear bands at around 23–35 kDa (Figure 4A, lane 3). After treatment with PNGase F to remove N-glycan, the smear band disappeared and a band at 33 kDa corresponding to de-N-glycosylated full-size protein became a major one (lane 1). The altered (p.Gly92Asp) protein in family A showed similar profiles (lanes 7 and 9), suggesting normal levels of PGAP3 bearing normally matured N-glycan. Consistently, on immunofluorescence microscopy,

Table 1. Summary of Clinical Findings in Individuals with *PGAP3* Mutations

	Individual				
Clinical Findings[a]	**V-1 (Family A)**	**V-2 (Family A)**	**V-3 (Family A)**	**II-1 (Family B)**	**II-1 (Family C)**
Ethnicity	Pakistani (Sargodha district of Punjab)	Pakistani (Sargodha district of Punjab)	Pakistani (Sargodha district of Punjab)	American (European descent)	Saudi-Arabian
Consanguinity	yes	yes	yes	no	yes
Age of last assessment (years)	17	8	4	10	2
OFC at birth	normal	normal	normal	normal	normal
OFC	−2 to −3 SDs	−2 to −3 SDs	−3 SDs	mean	mean
Height	normal	normal	normal	−4 SDs	normal
Weight	normal	normal	normal	−2 SDs	normal
Global developmental delay (HP:0001263)	yes	yes	yes	yes	yes
Motor delay (HP:0001270)	severe (unable to walk)	severe (unable to walk)	severe (unable to walk)	severe (walk with support at age of 3 years)	severe (unable to walk)
Speech and language development	none	none	none	none	none
Muscular hypotonia (HP:0001252)	yes	yes	yes	yes	yes
Seizures (HP:0001250)	yes	yes	no	yes	yes
Age of onset of seizures (years)	12	4	NA	4	1.5
Type of seizures	generalized tonic-clonic	generalized tonic-clonic	NA	tonic-clonic and cluster	myoclonic
Antiepileptic drugs	valproate	valproate	NA	rufinamide, pregabaline	valproate, levetiracetam
Behavioral abnormalities	involuntary midline hand movements, bruxism	involuntary midline hand movements, bruxism	involuntary midline hand movements, bruxism	no	hyperactivity
Apparent hypertelorism (HP:0000316)	yes	yes	yes	yes	yes
Upslanting palpebral fissures (HP:0000582)	yes	yes	yes	no	no
Broad nasal bridge (HP:0000431)	yes	yes	yes	yes	yes
Broad nasal tip	yes	yes	yes	yes	yes
Short nose (HP:0003196)	yes	yes	yes	yes	yes
Tented upper-lip vermilion (HP:0010804)	yes	yes	yes	yes	yes
Large, fleshy ear lobes (HP:0009748)	yes	yes	yes	no	yes
Cleft palate (HP:0000175)	yes	yes	no (high palate)	no	no
Brachytelephalangy (HP:0009882)	no	no	no	no	no
Serum total ALP (U/l) (HP:0003155)	739	1,407	1,452	926–2,000	928–1,370
Upper limit in ALP test (U/l)	525–600	525–600	525–600	400	386

(*Continued on next page*)

Table 1. ***Continued***

Clinical Findings[a]	Individual				
	V-1 (Family A)	V-2 (Family A)	V-3 (Family A)	II-1 (Family B)	II-1 (Family C)
Further anomalies	no	no	no	no	thin corpus callosum, dilated lateral ventricles
PGAP3 variants (RefSeq NM_033419.3)	homozygous c.275G>A (p.Gly92Asp)	homozygous c.275G>A (p.Gly92Asp)	homozygous c.275G>A p.Gly92Asp)	compound-heterozygous c.914A>G (p.Asp305Gly) and c.439dupC (p.Leu147Profs*16)	homozygous c.314C>G (p.Pro105Arg)

Abbreviations are as follows: ALP, alkaline phosphatase; OFC, occipitofrontal circumference; and NA, not applicable.
[a]Human phenotype ontology IDs are provided if applicable.

wild-type and p.Gly92Asp PGAP3 were found mainly in the Golgi and to a lesser extent in the ER (Figure 5, first and second rows). Only faint bands were seen with p.Leu147Profs*16 from family B, indicating that the level of altered protein was not significant (Figure 4C). The other family B substitution, p.Asp305Gly, showed a main band at 35 kDa (Figure 4A, lane 6) that was shifted to the 33 kDa de-N-glycosylated full-size protein after treatment with either PNGase F or Endo H, the latter of which eliminated only immature N-glycan (lanes 4 and 5). This profile indicated that the p.Asp305Gly altered protein had only immature ER-form N-glycan. Consistently, the altered

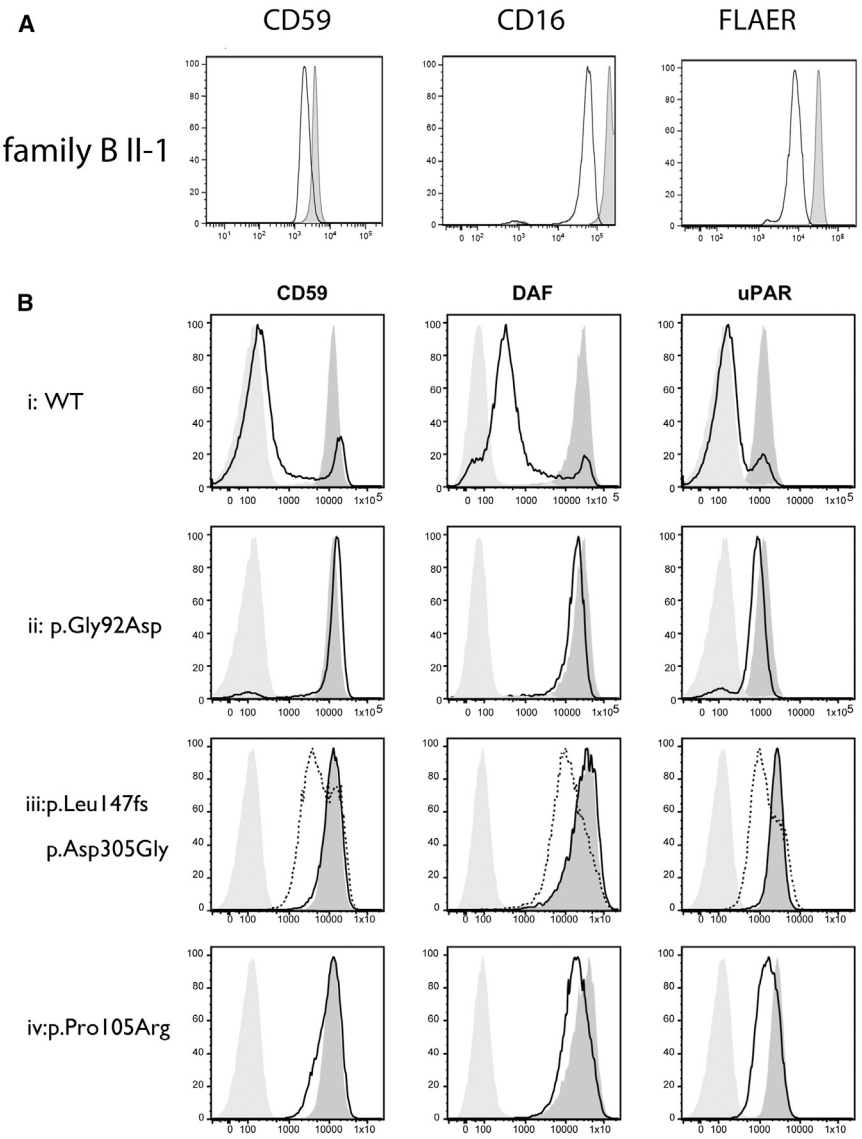

Figure 3. Flow Cytometric Analysis of Granulocyte Surface GPI-APs and Flow Cytometric Assay for Functions of Altered PGAP3

(A) Blood granulocytes from the affected individual in family B (solid line) were stained with anti-CD24 and anti-CD16 and fluorescence-labeled aerolysin (FLAER). The light-gray area represents a healthy control.

(B) *PGAP3* and *PGAP2* double-mutant CHO cells were transfected with *PGAP3* cDNA and 2 days later were stained for CD59, CD55 (DAF), and uPAR. (Bi) After transfection with wild-type *PGAP3* cDNA, the surface levels of three GPI-APs were severely reduced (solid lines). The dark area shows the original surface levels of GPI-APs on *PGAP3* and *PGAP2* double-mutant CHO cells, whereas the light gray area represents the isotype-matched control. (Bii) The *PGAP3* cDNA bearing mutation c.275G>A (p.Gly92Asp) in family A either did not reduce or only slightly reduced GPI-AP levels (solid lines). (Biii) The *PGAP3* cDNA bearing one mutation, c.439dupC (p.Leu147Profs*16), in family B did not reduce GPI-AP levels (solid lines), whereas that bearing the other mutation, c.914A>G (p.Asp305Gly), significantly reduced GPI-AP levels, indicating a hypomorphic mutant phenotype (dotted lines). (Biv) The *PGAP3* cDNA bearing mutation c.314C>G (p.Pro105Arg) in family C slightly reduced the levels of three GPI-APs, indicating a hypomorphic but very severe loss-of-function phenotype (solid lines).

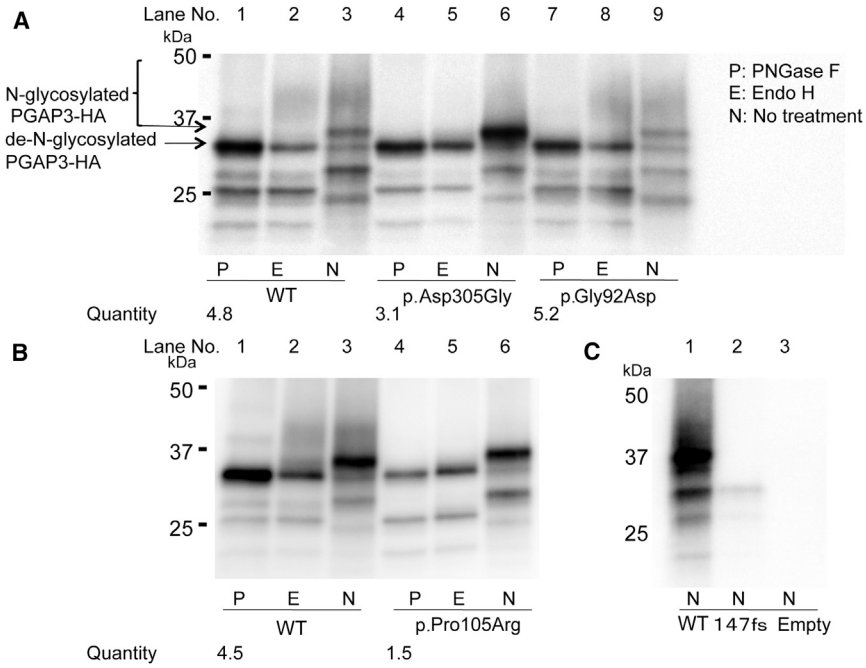

Figure 4. SDS-PAGE and Immunoblotting of HA-Tagged PGAP3

(A) Lanes 1–3, wild-type; lanes 4–6, p.Asp305Gly; lanes 7–9, p.Gly92Asp. Protein levels shown as quantity were normalized with the intensities of GAPDH for the loading control and luciferase activities for the transfection efficiencies. The antibody showed no reactivity in lysates from empty-vector-transfected cells.

(B) Lanes 1–3, wild-type; lanes 4–6, p.Pro105Arg.

(C) Lane 1, wild-type; lane 2, p.Leu147Profs*16; lane 3, empty vector. There are two N-glycosylation sites in PGAP3. The mature PGAP3 appears as a smear at 37–45 KDa (A, lane 3). This smear is sensitive to PNGase F, suggesting heterogeneous N-glycans. Bands seen below the 35 KDa position represent degradation products because they are not seen in the empty-vector transfectant (C, lane 3) or the transfectant with the truncated p.Leu147Profs*16 protein (C, lane 2). Abbreviations are as follows: N, no treatment; P, PNGase F treatment; and E, Endo H treatment.

protein was found in the ER, but not the Golgi (Figure 5, third row). Similarly, the p.Pro105Arg substitution in family C generated only an immature protein with ER-form N-glycan, as shown by a lack of a smear band at around 37–45 kDa (Figure 4B, lane 6) and a shift of the clear major band at 35 kDa to 33 kDa after Endo-H treatment (lanes 5 and 6). Consistent with these results, p.Pro105Arg PGAP3 was localized to the ER, but not to the Golgi (Figure 5, fourth row).

Therefore, the four substitutions that we describe had different effects on PGAP3, the Golgi-resident GPI-specific phospholipase A_2 consisting of an N-terminal luminal domain, seven transmembrane domains with conserved catalytic amino acids, and a C-terminal cytoplasmic tail (Figure S4). (1) The p.Gly92Asp substitution did not affect protein levels or Golgi localization, yet the altered protein had only negligible activity. Because Gly92 resides in a juxta membrane position on the luminal side, a negative charge caused by this substitution might interfere with the association between PGAP3 and GPI anchor substrate. (2) The p.Leu147Profs*16 protein was not detected significantly, consistent with nonsense-mediated mRNA degradation. (3) The p.Asp305Gly and p.Pro105Arg proteins were readily detectable but had immature N-glycan and were mislocalized in the ER. Asp305 resides in the cytoplasmic tail, whereas Pro105 resides in the first transmembrane domain. The cytoplasmic tail and the first transmembrane domain might be important for Golgi localization.

The characteristic biochemical phenotype of individuals with *PGAP3* deficiency is hyperphosphatasia, a sign of GPI-AP release from the cell surface. However, the reduction of GPI-AP levels is expected to depend on the cell type and species, as studies in *Pgap3*-knockout mice suggest.[24,25] In fact, flow cytometric analysis from the affected individual in family B demonstrated significant reduction in the cell-surface levels of GPI-APs in blood granulocytes (Figure 3A), whereas the CD59 surface levels in erythrocytes of an affected individual in family A were found to be normal. This confirms that GPI remodelling by PGAP3 is not essential for CD59 surface levels in erythrocytes, given that the GPI-anchor structure in erythrocytes maintains an unsaturated fatty acid at the sn2 position.[26]

The exact mechanism of release has yet to be characterized, but GPI-APs bearing unremodelled fatty acids are not associated well with lipid rafts.[17] This abnormal membrane distribution might affect the stability of GPI-APs, resulting in release from the cell surface. Although both PGAP3 and PGAP2 are involved in fatty acid remodeling, the above mechanism of hyperphosphatasia or GPI-AP release from *PGAP3*-deficient cells is different from that observed in *PGAP2*-deficient cells. In the latter cells, only the first reaction by PGAP3, elimination of unsaturated fatty acid, occurs and the resulting lyso-GPI intermediate is cleaved and released by a putative lyso-GPI-specific phospholipase D.[15]

In summary, we identified four different *PGAP3* mutations in three unrelated families by using two independent strategies. In family A, recruited on account of postnatal microcephaly, a combination of autozygosity mapping and exome sequencing identified a missense variant in *PGAP3* as the only likely candidate. In families B and C, mutations were uncovered in the same gene via a targeted sequencing approach in a cohort of individuals ascertained specifically for ID and hyperphosphatasia. In spite of the different approaches, the convergent findings, taken together with the segregation, the absence of these

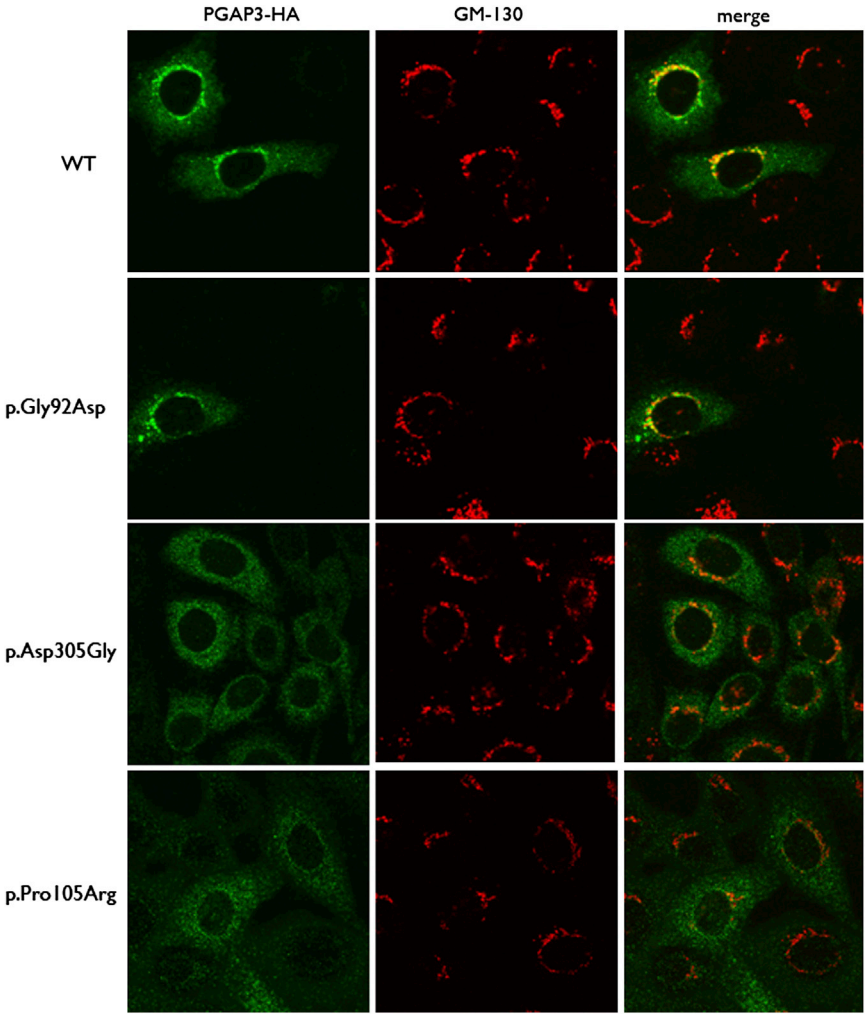

Figure 5. Subcellular Localization of HA-Tagged PGAP3 in CHO Cells
(First row) Wild-type.
(Second row) p.Gly92Asp in family A.
(Third row) p.Asp305Gly in family B.
(Fourth row) Pro105Arg in family C.
GM-130 is the Golgi marker. The relatively high levels of the ER form of HA-tagged wild-type PGAP3 seen in the top panels and also in lane 3 in Figure 4A might have been due to overexpression.

variants in suitable controls, phylogenetic conservation, and functional studies on CHO cell lines, provide strong evidence supporting the etiological role of these mutations. Along with *PGAP1* and *PGAP2*, *PGAP3* is responsible for the modification of the fatty acid residues on the GPI anchor in a maturation process that occurs in the ER and Golgi. Our results and previously reported data on *PGAP2* mutations suggest that impairment of fatty acid remodelling results in GPI-APs that are more prone to cleavage on the plasma membrane and clinical features that are similar to HPMRS. Our findings widen both the phenotypic and the genotypic spectra of hyperphosphatasia and ID syndromes that are caused by mutations in *PIGV, PIGO*, and *PGAP2* and suggest a heterogeneous etiology caused by impairment of late GPI-anchor synthesis and the GPI-AP-maturation pathway. These functional mutations define this condition as a CDG, PGAP3-CDG. In contrast to classical CDGs, which affect N-glycosylation and O-glycosylation, or both, defects in the GPI-anchor-biosynthesis pathway cannot be detected with a transferrin or APOCIII glycosylation assay. This underlines the importance of comprehensive genetic testing of individuals with suspected CDGs.

Supplemental Data

Supplemental Data include four figures and two tables and can be found with this article online at http://www.cell.com/AJHG.

Acknowledgments

This work was supported by the National Institute for Health Research (NIHR) Biomedical Research Centre Oxford with funding from the Department of Health's NIHR Biomedical Research Centres funding scheme. The views expressed in this publication are those of the authors and not necessarily those of the Department of Health. The work was also supported by a grant from the German Ministry of Research and Education to S.M. (0313911), by Deutsche Forschungsgemeinschaft grants to P.M.K. (KR 3985/1-1) and S.M. (SFB 665), and by grants from the Ministry of Education, Culture, Sports, Science, and Technology and the Ministry of Health, Labour, and Welfare of Japan to Y.M. and T.K. We thank the High-Throughput Genomics Group at the Wellcome Trust Centre for Human Genetics (funded by Wellcome Trust grant reference 090532/Z/09/Z and Medical Research Council Hub grant G0900747 91070) for generating the sequencing data, John Broxholme for assisting with downloading BAM files from the 1000 Genomes Project, Kevin Leyden for performing flow cytometry, Christian Babbs for sharing DNA from Arabic

controls, and Kana Miyanagi for assisting in functional analysis of PGAP3. We would also like to thank all three families for their participation in this study and the 500 Whole-Genome Sequences Consortium and Illumina for use of the in-house database of variant calls for 274 individuals.

Received: September 25, 2013
Accepted: December 11, 2013
Published: January 16, 2014

Web Resources

The URLs for data presented herein are as follows:

1000 Genomes, http://www.1000genomes.org/
ANNOVAR, http://www.openbioinformatics.org/annovar/
Burrows-Wheeler Aligner, http://bio-bwa.sourceforge.net/
ClustalW, http://www.clustal.org/clustal2/
Coriell Cell Repositories, http://ccr.coriell.org/
dbSNP, http://www.ncbi.nlm.nih.gov/snp/
GATK, http://www.broadinstitute.org/gatk/index.php
GeneTalk, http://www.gene-talk.de
Ingenuity, https://variants.ingenuity.com/MutationsinPGAP3causeARID
HomozygosityMapper, http://www.homozygositymapper.org/
KEGG: Kyoto Encyclopedia of Genes and Genomes, http://www.genome.jp/kegg/
LifeScope, http://www.lifetechnologies.com/lifescope.html
MutationTaster, http://www.mutationtaster.org
NHLBI Exome Sequencing Project (ESP) Exome Variant Server, http://evs.gs.washington.edu/EVS/
Online Mendelian Inheritance in Man (OMIM), http://www.omim.org
Oxford Brain Abnormality Research Group, http://www.brainabnormalities.org.uk
Platypus, http://www.well.ox.ac.uk/platypus
PolyPhen-2, http://genetics.bwh.harvard.edu/pph2/
SIFT, http://sift.jcvi.org/
UCSC Genome Browser, http://www.genome.ucsc.edu

References

1. Fujita, M., and Kinoshita, T. (2012). GPI-anchor remodeling: potential functions of GPI-anchors in intracellular trafficking and membrane dynamics. Biochim. Biophys. Acta *1821*, 1050–1058.
2. McKean, D.M., and Niswander, L. (2012). Defects in GPI biosynthesis perturb Cripto signaling during forebrain development in two new mouse models of holoprosencephaly. Biol. Open *1*, 874–883.
3. Park, S., Lee, C., Sabharwal, P., Zhang, M., Meyers, C.L., and Sockanathan, S. (2013). GDE2 promotes neurogenesis by glycosylphosphatidylinositol-anchor cleavage of RECK. Science *339*, 324–328.
4. Jaeken, J. (2011). Congenital disorders of glycosylation (CDG): it's (nearly) all in it!. J. Inherit. Metab. Dis. *34*, 853–858.
5. Nozaki, M., Ohishi, K., Yamada, N., Kinoshita, T., Nagy, A., and Takeda, J. (1999). Developmental abnormalities of glycosylphosphatidylinositol-anchor-deficient embryos revealed by Cre/loxP system. Lab. Invest. *79*, 293–299.
6. Johnston, J.J., Gropman, A.L., Sapp, J.C., Teer, J.K., Martin, J.M., Liu, C.F., Yuan, X., Ye, Z., Cheng, L., Brodsky, R.A., and Biesecker, L.G. (2012). The phenotype of a germline mutation in PIGA: the gene somatically mutated in paroxysmal nocturnal hemoglobinuria. Am. J. Hum. Genet. *90*, 295–300.
7. Ng, B.G., Hackmann, K., Jones, M.A., Eroshkin, A.M., He, P., Wiliams, R., Bhide, S., Cantagrel, V., Gleeson, J.G., Paller, A.S., et al. (2012). Mutations in the glycosylphosphatidylinositol gene PIGL cause CHIME syndrome. Am. J. Hum. Genet. *90*, 685–688.
8. Almeida, A.M., Murakami, Y., Layton, D.M., Hillmen, P., Sellick, G.S., Maeda, Y., Richards, S., Patterson, S., Kotsianidis, I., Mollica, L., et al. (2006). Hypomorphic promoter mutation in PIGM causes inherited glycosylphosphatidylinositol deficiency. Nat. Med. *12*, 846–851.
9. Maydan, G., Noyman, I., Har-Zahav, A., Neriah, Z.B., Pasmanik-Chor, M., Yeheskel, A., Albin-Kaplanski, A., Maya, I., Magal, N., Birk, E., et al. (2011). Multiple congenital anomalies-hypotonia-seizures syndrome is caused by a mutation in PIGN. J. Med. Genet. *48*, 383–389.
10. Kvarnung, M., Nilsson, D., Lindstrand, A., Korenke, G.C., Chiang, S.C., Blennow, E., Bergmann, M., Stödberg, T., Mäkitie, O., Anderlid, B.M., et al. (2013). A novel intellectual disability syndrome caused by GPI anchor deficiency due to homozygous mutations in PIGT. J. Med. Genet. *50*, 521–528.
11. Krawitz, P.M., Murakami, Y., Hecht, J., Krüger, U., Holder, S.E., Mortier, G.R., Delle Chiaie, B., De Baere, E., Thompson, M.D., Roscioli, T., et al. (2012). Mutations in PIGO, a member of the GPI-anchor-synthesis pathway, cause hyperphosphatasia with mental retardation. Am. J. Hum. Genet. *91*, 146–151.
12. Krawitz, P.M., Schweiger, M.R., Rödelsperger, C., Marcelis, C., Kölsch, U., Meisel, C., Stephani, F., Kinoshita, T., Murakami, Y., Bauer, S., et al. (2010). Identity-by-descent filtering of exome sequence data identifies PIGV mutations in hyperphosphatasia mental retardation syndrome. Nat. Genet. *42*, 827–829.
13. Murakami, Y., Kanzawa, N., Saito, K., Krawitz, P.M., Mundlos, S., Robinson, P.N., Karadimitris, A., Maeda, Y., and Kinoshita, T. (2012). Mechanism for release of alkaline phosphatase caused by glycosylphosphatidylinositol deficiency in patients with hyperphosphatasia mental retardation syndrome. J. Biol. Chem. *287*, 6318–6325.
14. Hansen, L., Tawamie, H., Murakami, Y., Mang, Y., ur Rehman, S., Buchert, R., Schaffer, S., Muhammad, S., Bak, M., Nöthen, M.M., et al. (2013). Hypomorphic mutations in PGAP2, encoding a GPI-anchor-remodeling protein, cause autosomal-recessive intellectual disability. Am. J. Hum. Genet. *92*, 575–583.
15. Krawitz, P.M., Murakami, Y., Rieß, A., Hietala, M., Krüger, U., Zhu, N., Kinoshita, T., Mundlos, S., Hecht, J., Robinson, P.N., and Horn, D. (2013). PGAP2 mutations, affecting the GPI-anchor-synthesis pathway, cause hyperphosphatasia with mental retardation syndrome. Am. J. Hum. Genet. *92*, 584–589.
16. Tashima, Y., Taguchi, R., Murata, C., Ashida, H., Kinoshita, T., and Maeda, Y. (2006). PGAP2 is essential for correct processing and stable expression of GPI-anchored proteins. Mol. Biol. Cell *17*, 1410–1420.
17. Maeda, Y., Tashima, Y., Houjou, T., Fujita, M., Yoko-o, T., Jigami, Y., Taguchi, R., and Kinoshita, T. (2007). Fatty acid remodeling of GPI-anchored proteins is required for their raft association. Mol. Biol. Cell *18*, 1497–1506.
18. Najmabadi, H., Hu, H., Garshasbi, M., Zemojtel, T., Abedini, S.S., Chen, W., Hosseini, M., Behjati, F., Haas, S., Jamali, P.,

et al. (2011). Deep sequencing reveals 50 novel genes for recessive cognitive disorders. Nature *478*, 57–63.
19. Lunter, G., and Goodson, M. (2011). Stampy: a statistical algorithm for sensitive and fast mapping of Illumina sequence reads. Genome Res. *21*, 936–939.
20. Kamphans, T., and Krawitz, P.M. (2012). GeneTalk: an expert exchange platform for assessing rare sequence variants in personal genomes. Bioinformatics *28*, 2515–2516.
21. Thompson, M.D., Roscioli, T., Marcelis, C., Nezarati, M.M., Stolte-Dijkstra, I., Sharom, F.J., Lu, P., Phillips, J.A., Sweeney, E., Robinson, P.N., et al. (2012). Phenotypic variability in hyperphosphatasia with seizures and neurologic deficit (Mabry syndrome). Am. J. Med. Genet. A. *158A*, 553–558.
22. Heinrich, V., Kamphans, T., Stange, J., Parkhomchuk, D., Hecht, J., Dickhaus, T., Robinson, P.N., and Krawitz, P.M. (2013). Estimating exome genotyping accuracy by comparing to data from large scale sequencing projects. Genome Med. *5*, 69.
23. Kamphans, T., Sabri, P., Zhu, N., Heinrich, V., Mundlos, S., Robinson, P.N., Parkhomchuk, D., and Krawitz, P.M. (2013). Filtering for compound heterozygous sequence variants in non-consanguineous pedigrees. PLoS ONE *8*, e70151.
24. Murakami, H., Wang, Y., Hasuwa, H., Maeda, Y., Kinoshita, T., and Murakami, Y. (2012). Enhanced response of T lymphocytes from Pgap3 knockout mouse: Insight into roles of fatty acid remodeling of GPI anchored proteins. Biochem. Biophys. Res. Commun. *417*, 1235–1241.
25. Wang, Y., Murakami, Y., Yasui, T., Wakana, S., Kikutani, H., Kinoshita, T., and Maeda, Y. (2013). Significance of glycosylphosphatidylinositol-anchored protein enrichment in lipid rafts for the control of autoimmunity. J. Biol. Chem. *288*, 25490–25499.
26. Rudd, P.M., Morgan, B.P., Wormald, M.R., Harvey, D.J., van den Berg, C.W., Davis, S.J., Ferguson, M.A., and Dwek, R.A. (1998). The glycosylation of the complement regulatory protein, human erythrocyte CD59. Adv. Exp. Med. Biol. *435*, 153–162.